Electronic Supplementary Information (ESI) for Chemical Communications

Reduced Mo-doped $NiCo_2O_4$ with rich oxygen vacancies as advanced electrode material in supercapacitors

Chengchao Wang, Xingyue Wu, Yong Qin and Yong Kong*

Jiangsu Key Laboratory of Advanced Materials and Technology, School of Petrochemical Engineering, Changzhou University, Changzhou 213164, China

Email address: yzkongyong@cczu.edu.cn

Experimental section

Reagents and apparatus. Nickel nitrate hexahydrate ($Ni(NO_3)_2·6H_2O$), cobalt nitrate hexahydrate ($Co(NO_3)_2·6H_2O$), sodium borohydride ($NaBH_4$), potassium hydroxide (KOH) and anhydrous alcohol were purchased from Sinopharm Chemical Reagent Co., Ltd. (Shanghai, China). Sodium molybdate dihydrate ($Na_2MoO_4·2H_2O$) was obtained from Aladdin Chemistry Co., Ltd. (Shanghai, China). Urea was received from Shanghai Macklin Biochemical Technology Co., Ltd. (Shanghai, China). All aqueous solutions were prepared with ultrapure water (18.2 MΩ·cm, Millipore).

Scanning electron microscopy (SEM) and transmission electron microscopy (TEM) characterizations were conducted with a Supra55 field-emission scanning electron microscope (Zeiss, Germany) and a JEM 2100 transmission electron microscope (JEOL, Japan), respectively. The X-ray diffraction (XRD) patterns of different samples were recorded on a D/max 2500PC diffractometer (Rigaku, Japan). The N_2 adsorption/desorption isotherms as well as the pore size distributions of different samples were determined by using an ASAP 2010 specific surface area and pore size analyzer (Micromeritics, USA). The X-ray photoelectron spectroscopy (XPS) of $NiCo_2O_4$, Mo-$NiCo_2O_4$ and R-Mo-$NiCo_2O_4$ was conducted with an ESCALAB 250Xi X-ray photoelectron spectrometer (Thermo Fisher Scientific, USA). The electron paramagnetic resonance (EPR) spectra of $NiCo_2O_4$, Mo-$NiCo_2O_4$ and R-Mo-$NiCo_2O_4$ were recorded by means of an EMXmicro EPR spectrometer (Bruker, Germany). The electrical conductivities of different samples were measured by a SZT-2A four-probe instrument purchased from Tongchuang Electronics Co., Ltd. (Suzhou, China). All electrochemical data including cyclic voltammograms (CVs), galvanostatic charge/discharge (GCD) curves and electrochemical impedance spectroscopy (EIS) were obtained on a CHI660D electrochemical workstation (Shanghai Chenhua Instruments Co. Ltd., China).

Synthesis of Mo doped NiCo-LDH (Mo-NiCo-LDH). The synthesis of NiCo-LDH has been reported previously,[1] and here Mo-NiCo-LDH was synthesized by the same method except for the addition of $Na_2MoO_4·2H_2O$ as the Mo source. In a typical procedure, 6 mmol of $Co(NO_3)_2·6H_2O$, 3 mmol of $Ni(NO_3)_2·6H_2O$, 18 mmol of urea and 0.3 mmol of $Na_2MoO_4·2H_2O$ were dissolved in the mixture of 60 mL anhydrous alcohol and 20 mL of water under sonication, which was then transferred into a 100 mL

Teflon-lined stainless-steel autoclave. The autoclave was sealed and maintained at 120 °C for 8 h. After that, the solvothermal products were washed with water and anhydrous alcohol for several times and dried at 60 °C for 12 h, and Mo-NiCo-LDH was obtained. For control experiments, NiCo-LDH was also synthesized by the same procedures without the addition of $Na_2MoO_4 \cdot 2H_2O$.

Synthesis of Mo-doped $NiCo_2O_4$ (Mo-$NiCo_2O_4$). One hundred milligrams of the as-synthesized Mo-NiCo-LDH were placed into a crucible and calcined at 350 °C in an air atmosphere (oxidation) for 3 h in a muffle furnace, and Mo-$NiCo_2O_4$ was obtained. For control experiments, $NiCo_2O_4$ was also synthesized by calcining NiCo-LDH under the same conditions.

Synthesis of reduced Mo-doped $NiCo_2O_4$ (R-Mo-$NiCo_2O_4$). One hundred milligrams of the above Mo-$NiCo_2O_4$ was dispersed in 60 mL of 1.0 M $NaBH_4$ solution under sonication. After 30 min of reduction at room temperature, the products (R-Mo-$NiCo_2O_4$) were centrifugally separated, washed with water and anhydrous alcohol for several times, and dried at 60 °C for 12 h. The production yield of the R-Mo-$NiCo_2O_4$ was calculated to be 46%.

Electrochemical measurements. All the electrochemical measurements were carried out in a conventional three-electrode cell consisting of a glassy carbon electrode (GCE, 3 mm in diameter) modified with different active materials as the working electrode, a platinum plate (10 × 5 mm) as the counter electrode and a KCl saturated calomel electrode (SCE) as the reference electrode. The electrolyte used in these electrochemical measurements was 2.0 M KOH solution. The working electrode was constructed by dropping 10 μL of the dispersion of different active materials (2 mg mL^{-1}) onto the surface of the GCE (loading capacity: 284 μg cm^{-2}) and dried in ambient air. The thickness of the active materials on the GCE surface was measured to be ~0.02 mm.

The CVs were acquired over the potential range between 0 and 0.5 V, and the GCD curves were recorded over the potential range between −0.2 and 0.4 V. The cyclic stability was investigated by repeating the GCD testing at a current density of 10 A g^{-1}. The EIS of different active materials was collected in the frequency range from 10^5 to 0.01 Hz at an open circuit potential of 0.1 V, and the equivalent circuit was simulated by the ZSimpWin software.

Calculation of specific capacity. The specific capacity of different active materials can be calculated from the GCD curves according to the following formula: $C_m = \frac{I \times t}{m}$, where C_m represents the specific capacity (mAh g^{-1}), I represents the current (mA), t represents the discharge time (h), and m represents the mass of the active materials (g).[2]

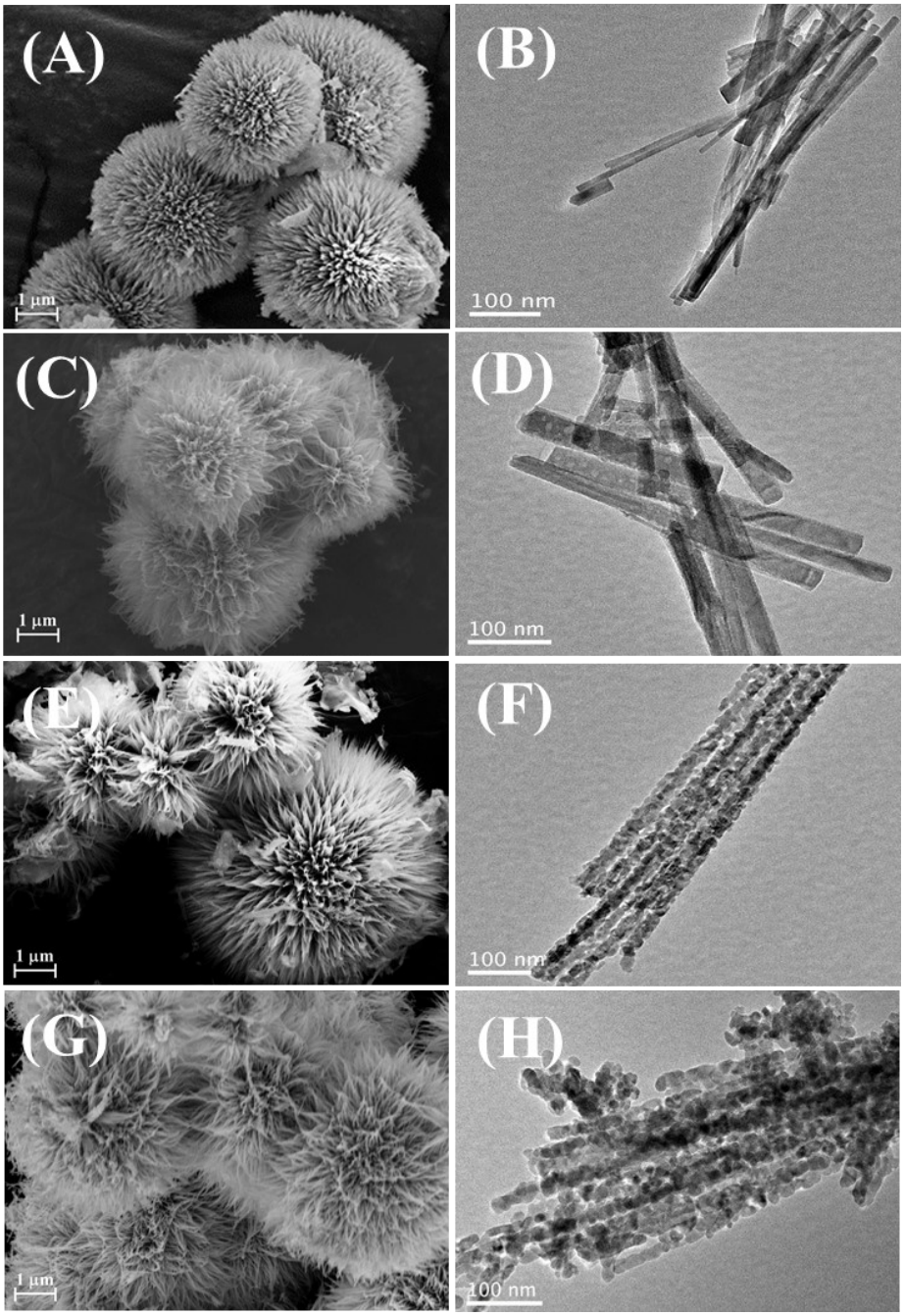

Figure S1 SEM and TEM images of NiCo-LDH (A, B), Mo-NiCo-LDH (C, D), $NiCo_2O_4$ (E, F) and Mo-$NiCo_2O_4$ (G, H).

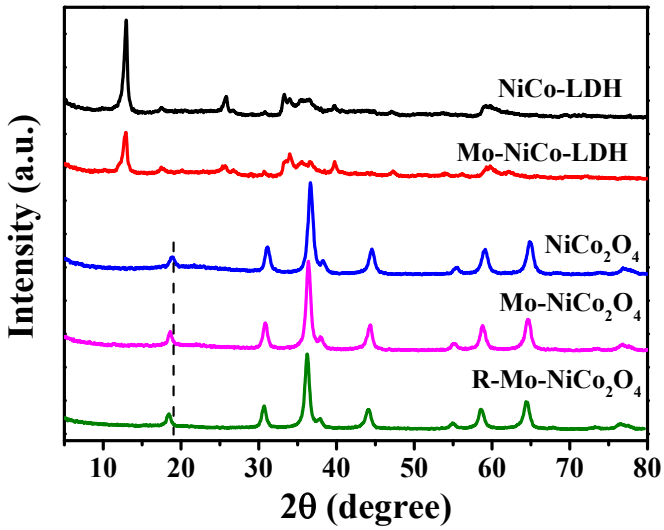

Figure S2 XRD patterns of NiCo-LDH, Mo-NiCo-LDH, $NiCo_2O_4$, Mo-$NiCo_2O_4$ and R-Mo-$NiCo_2O_4$.

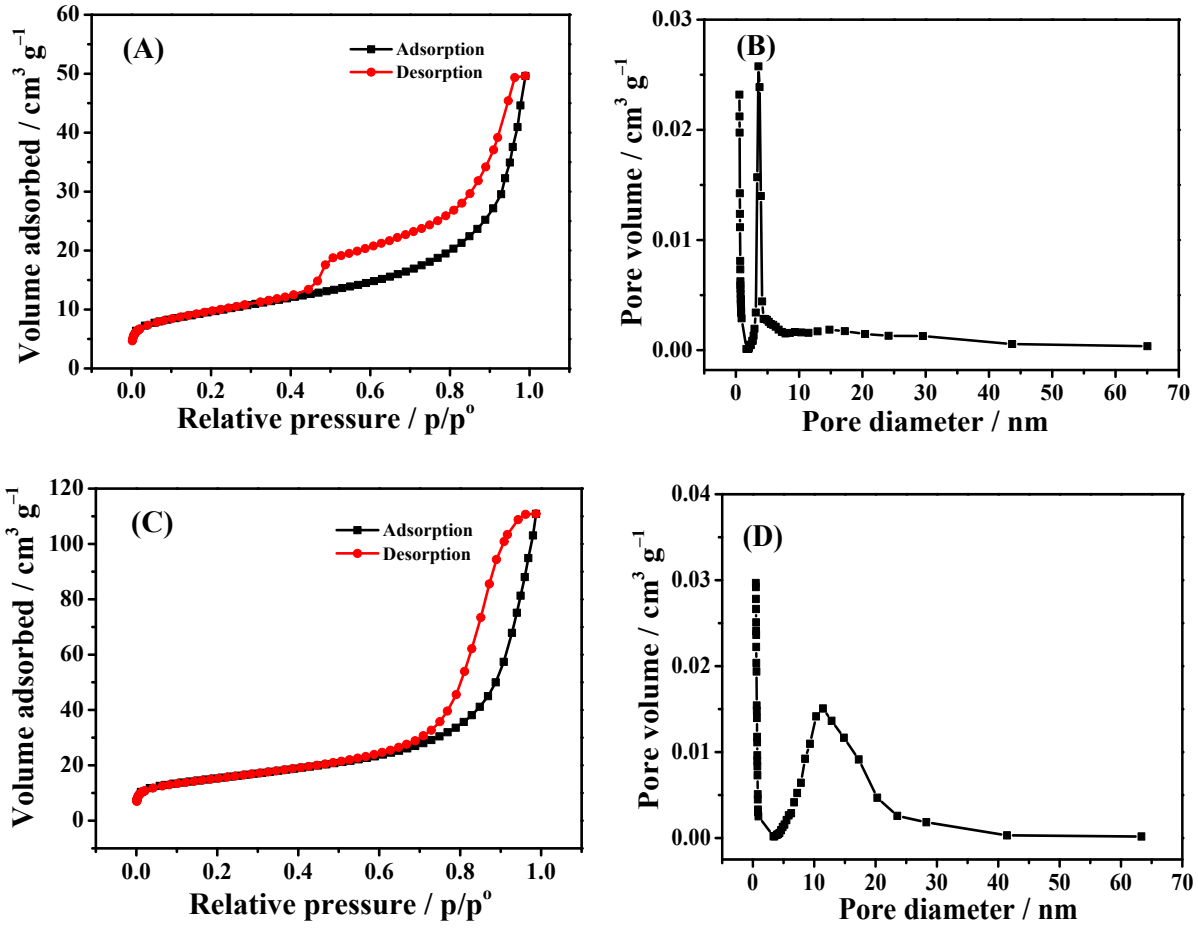

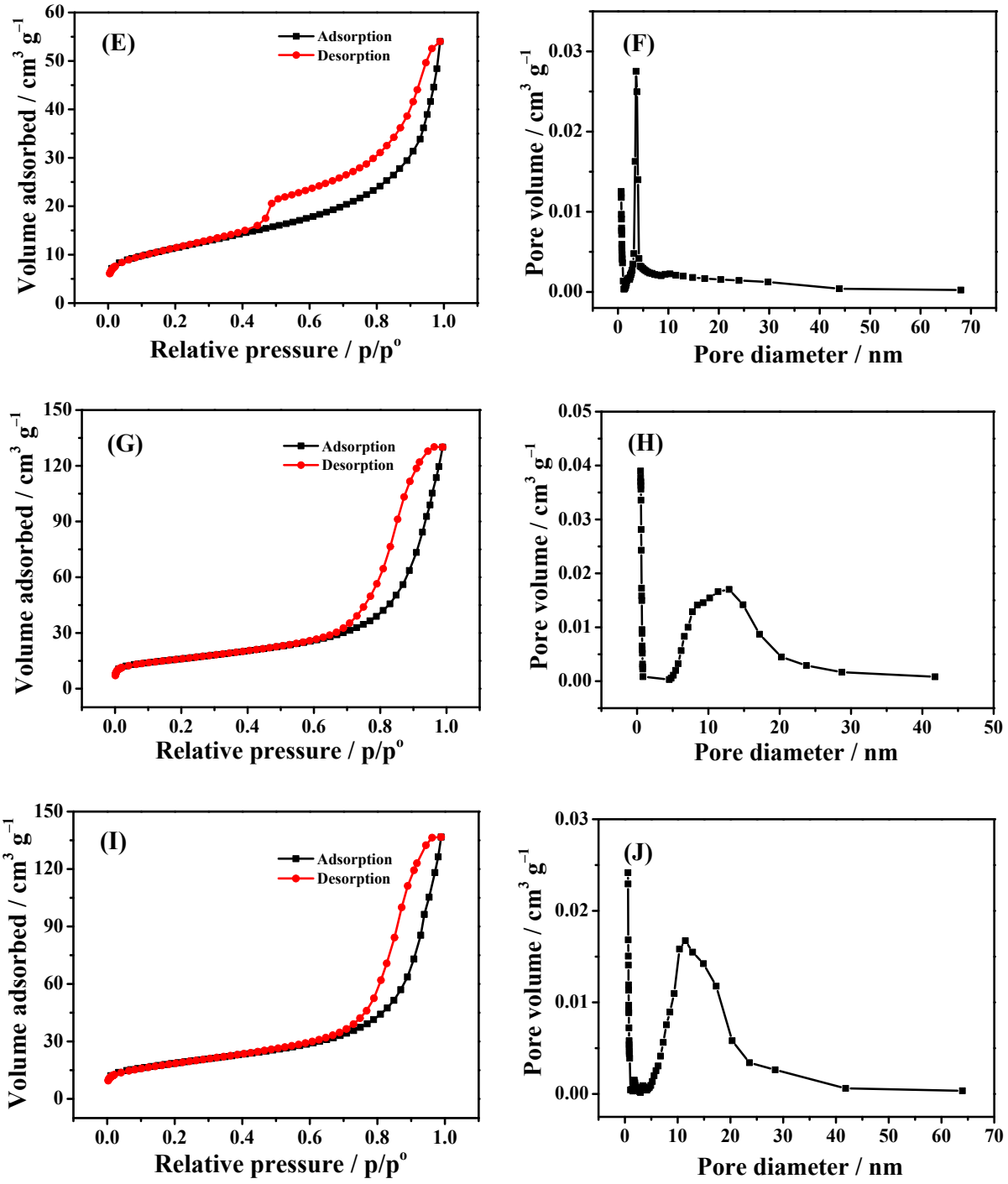

Figure S3 N_2 adsorption/desorption isotherms and pore size distributions of NiCo-LDH (A, B), Mo-NiCo-LDH (C, D), $NiCo_2O_4$ (E, F), Mo-$NiCo_2O_4$ (G, H) and R-Mo-$NiCo_2O_4$ (I, J).

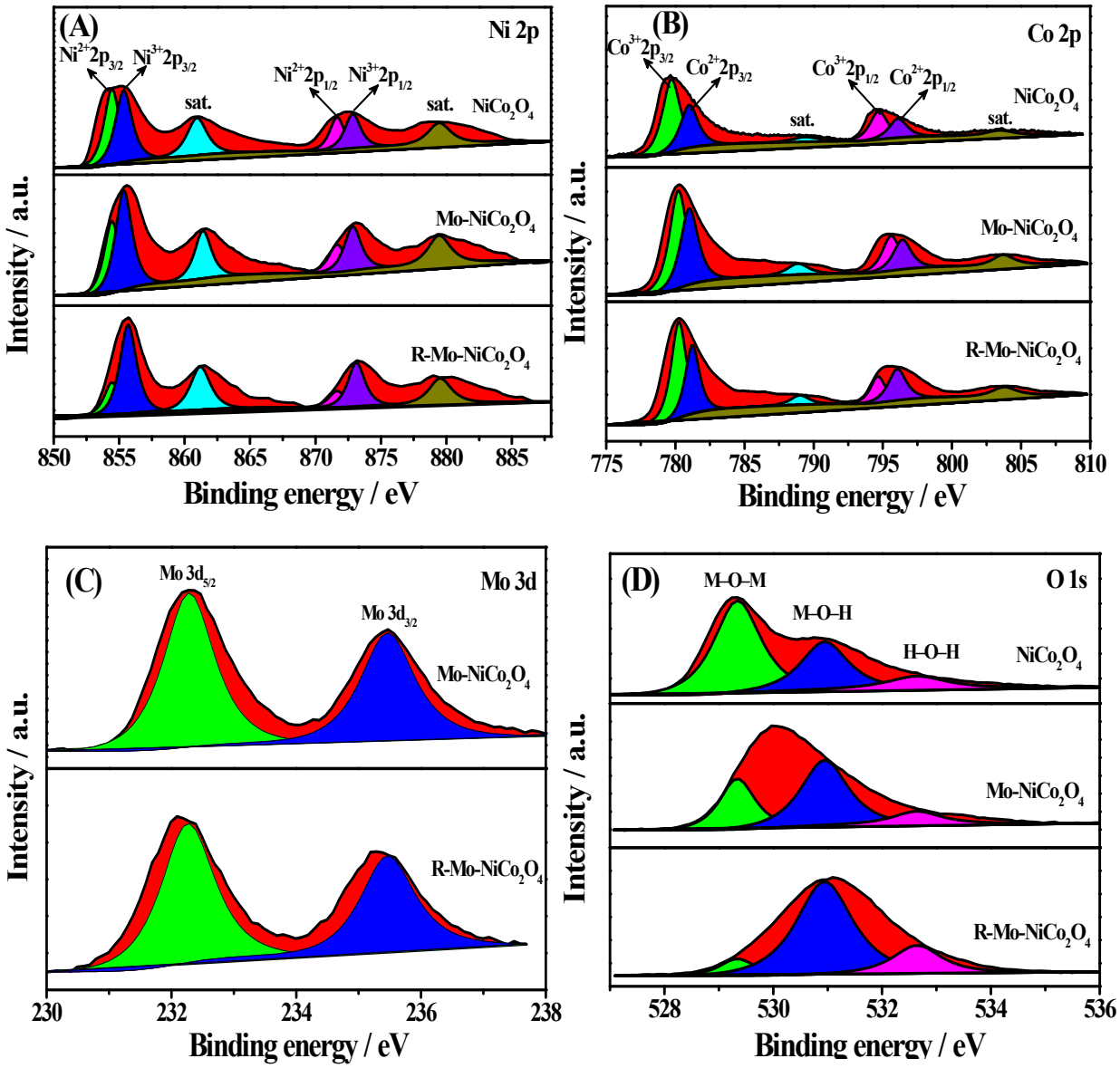

Figure S4 High-resolution XPS spectra of Ni 2p (A), Co 2p (B), Mo 3d (C) and O 1s (D) of $NiCo_2O_4$, Mo-$NiCo_2O_4$ and R-Mo-$NiCo_2O_4$.

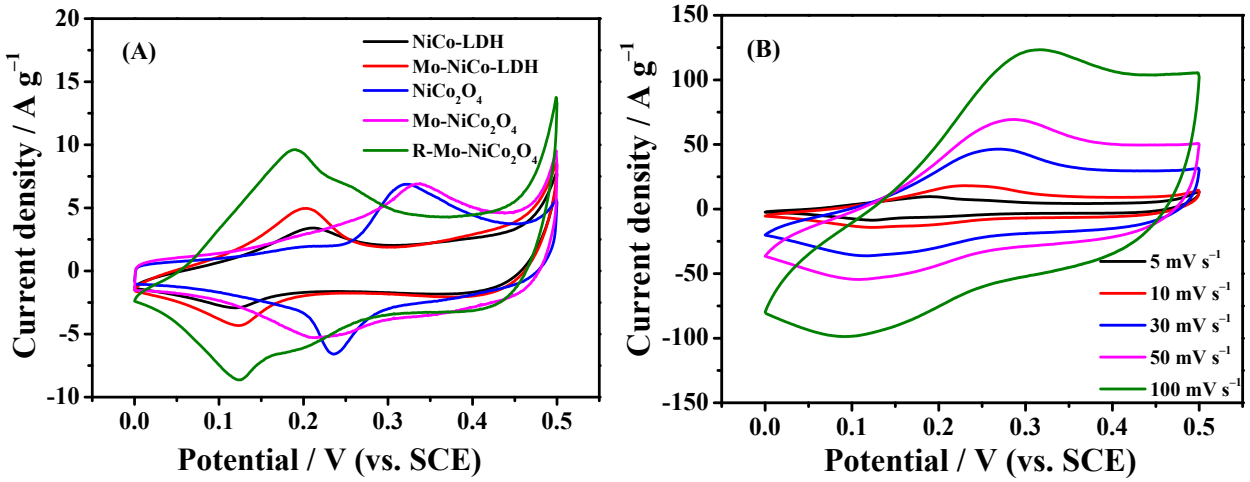

Figure S5 (A) Cyclic voltammograms of GCE modified with different active materials in 2.0 M KOH at the scan rate of 5 mV s^{-1}. (B) Cyclic voltammograms of R-Mo-$NiCo_2O_4$ modified GCE in 2.0 M KOH at different scan rates.

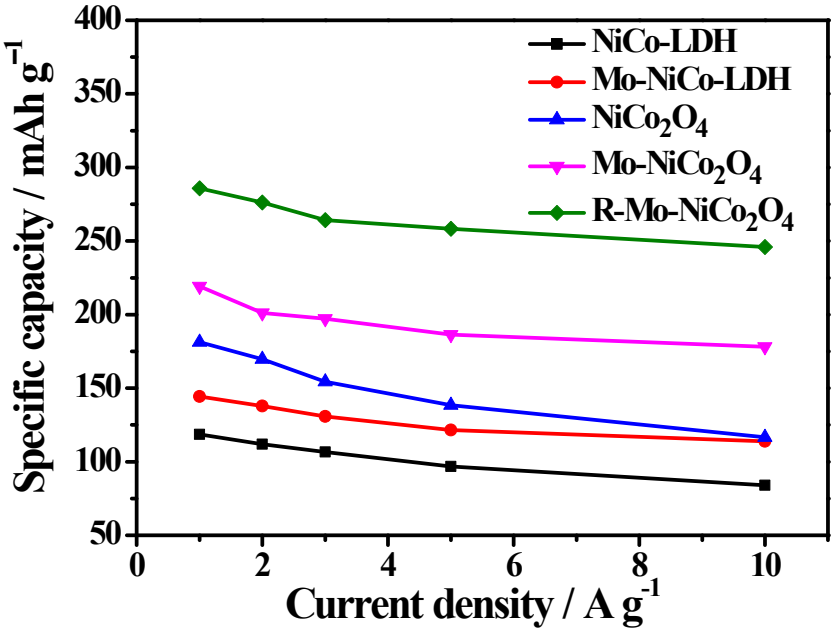

Figure S6 Specific capacities of GCE modified with different active materials in 2.0 M KOH at different current densities.

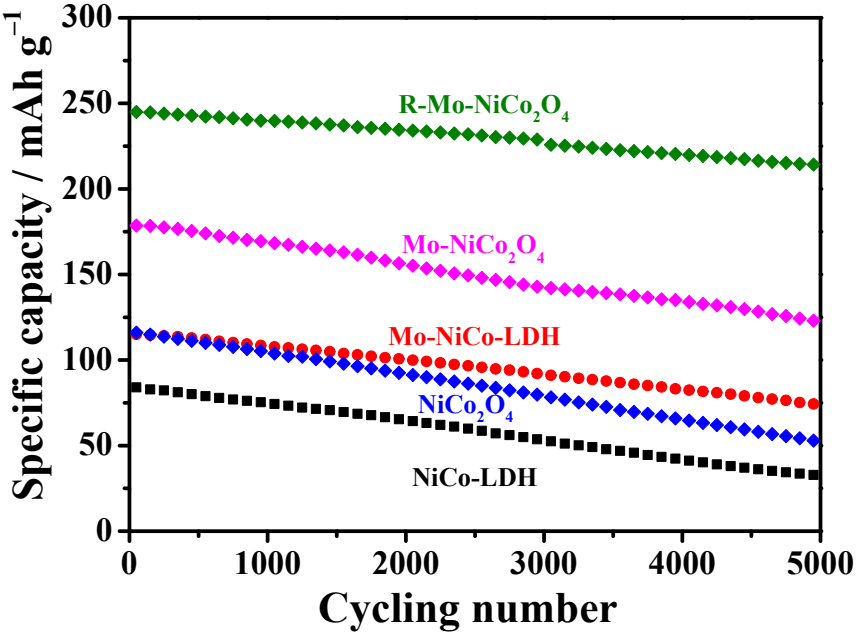

Figure S7 Cyclic stability of GCE modified with different active materials in 2.0 M KOH at the current density of 10 A g^{-1}.

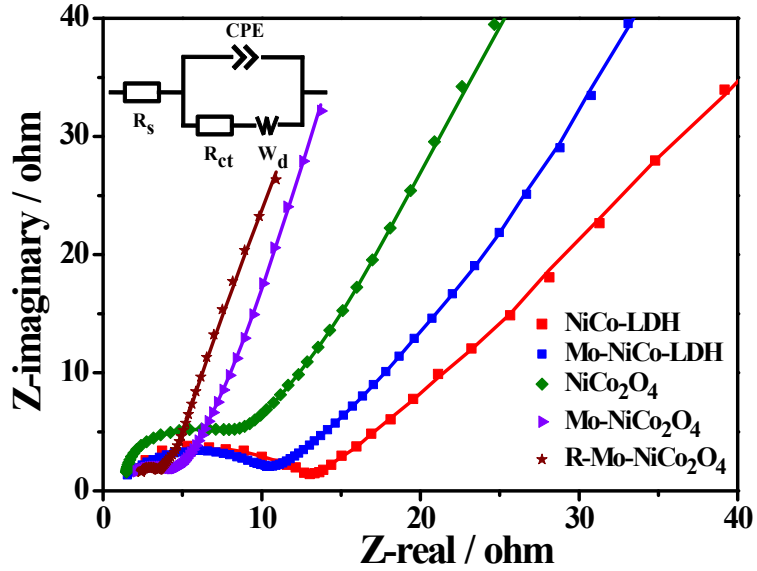

Figure S8 Nyquist plots of GCE modified with different active materials in 2.0 M KOH. Inset is the corresponding equivalent circuit, where R_s represents the ohmic resistance of electrolyte and the internal resistance of electrode, R_{ct} represents the interfacial charge transfer resistance, W_d represents the Warburg resistance, and CPE represents the constant phase element.

Table S1 Performance comparison with previous results at the current density of 1 A g^{-1}.

Sample	Capacity	Electrolyte	Reference
Co_3O_4	135.8 mAh g^{-1}	2 M KOH	3
$ZnCo_2O_4$	78.9 mAh g^{-1}	2 M KOH	4
$FeCo_2O_4$	52.4 mAh g^{-1}	1 M KOH	5
Ce-$NiMoO_4$	107.0 mAh g^{-1}	1 M KOH	6
R-Mo-$NiCo_2O_4$	285.8 mAh g^{-1}	2 M KOH	This work

Table S2 Electrical conductivities of different active materials.

Active materials	Electrical conductivity (S cm^{-1})
NiCo-LDH	28.3
Mo-NiCo-LDH	68.4
$NiCo_2O_4$	128.6
Mo-$NiCo_2O_4$	386.7
R-Mo-$NiCo_2O_4$	1258.3

References

1 H. Y. Liang, J. H. Lin, H. Jia, S. L. Chen, J. L. Qi, J. Cao, T. S. Lin, W. D. Fei and J. C. Feng, *J. Mater. Chem. A*, 2018, **6**, 15040.

2 C. C. Wang, W. G. Zheng, Z. Wang, Z. Z. Yin, Y. Qin and Y. Kong, *J. Electroanal. Chem.*, 2021, **901**, 115759.

3 S. H. Yang, Y. Y. Liu, Y. F. Hao, X. P. Yang, W. A. Goddard, X. L. Zhang and B. Q. Cao, *Adv. Sci*., 2018, **5**, 1700659.

4 Y. Y. Shang, T. Xie, C. L. Ma, L. H. Su, Y. S. Gai, J. Liu and L. Y. Gong, *Electrochim. Acta*, 2018, **286**, 103.

5 X. Liu, F. X. Wei, Y. W. Sui, J. Q. Qi, Y. Z. He and Q. K. Meng, *J. Alloys Compd*., 2018, **735**, 1339.

6 S. Z. Cui, F. Q. Wang, K. J. Sun, X. Wang, Q. Z. Hu, H. Peng, G. F. Ma and Z. Q. Lei, *J. Phys. Chem*. *C*, 2021, **125**, 18129.